Ion Propulsion Systems for Spacecraft

PAUL D. READER* AND WILLIAM R. MICKELSEN†
NASA Lewis Research Center, Cleveland, Ohio

Performance characteristics and power requirements of existing electron-bombardment thrustors are presented in a form useful to electric-propulsion-system analysis and design. This information is based on experimental operation of laboratory thrustor modules of from 5–50 cm in diam and module and array power levels of up to 30 kw. Static and dynamic controls characteristics of electron-bombardment thrustors are summarized. From these data, it is evident that no serious problems should arise in control-system design. A thrustor circuit design is described which suppresses electric breakdowns to a magnitude sufficiently small to eliminate damaging interaction between the thrustor and the power-conversion system. This circuit design is based on data obtained in operation of single thrustor modules and large thrustor arrays. It is shown that power-conversion and thrustor weights and performance penalties could reduce the payload of a 500-kw, 28,500-lb Mars-orbiter vehicle by 5000 to 9000 lb.

Introduction

ELECTRIC propulsion research and development has reached a point where serious consideration must be given to details of the over-all propulsion system. Some preliminary mission analyses have shown that weights and performance penalties of system components can severely reduce the payload capacity of electric spacecraft. It is the intent of this paper to present the performance and power requirements of electron-bombardment thrustors and to discuss problems of integration of these thrustors into the over-all vehicle and the propulsion system.

Thrust is produced by electron-bombardment thrustors through the electrostatic acceleration of a charged atomic propellant. The primary electric power to the ion thrustor must be direct current in the range of 3000–10,000 v for specific impulses of interest for lunar and near-interplanetary missions. It is expected that power output from the primary powerplant will be converted into d.c. electric power through a power-conditioning system with appropriate switchgear and controls.

The efficiency of the mercury-ion electron-bombardment thrustor is approaching the maximum that can be expected.[1] Further increases might be possible with heavy-molecule ions or charged colloidial particles as the propellant instead of the atomic ions currently being used.[2,3] Desired lifetimes (of the order of 10,000 hr) have not yet been reached, but present knowledge indicates that such lifetimes should be obtainable.[3] The electron-bombardment thrustor lends itself well for usage in a variety of propulsion systems because the size of a given module can be scaled.[4] To date, efficient operation has been obtained with thrustor modules from 5–50 cm in exhaust-beam diameter.

Possible thrustor applications range from small single-module thrustors for attitude control of satellites to multimegawatt arrays of thrustor modules for primary propulsion of large manned vehicles. From the systems viewpoint, the problems associated with this range of possible applications are vastly different. For example, a small thrustor with an exhaust-beam power of about 100 w is sufficient for attitude control of a 500-lb synchronous satellite.[5] Because only one thrustor of the attitude-control system (composed of several similar thrustors pointing in different directions) would be thrusting at any given time, the solar-cell power supply and d.c.-d.c. power-conditioning equipment can be closely matched to the power demands of the thrustor. Power interruption, arc suppression, and control functions may be accomplished in any one of a variety of ways as well as in the primary or secondary legs of the power-conditioning system. The maximum power loads are well within the capabilities of available solid-state components.

On the other hand, multimodule arrays of thrustors for primary propulsion could have power levels in the megawatt range. Power interruption, arc suppression, and control functions must be accomplished at each module because the whole propulsion system cannot be shut down for a single malfunctioning or faulted thrustor. The capacity of the system would allow serious, if not catastrophic, damage to be done to a malfunctioning component (or to the whole system) if electrical protection were not provided. A thrustor array for primary propulsion, therefore, requires high-current, high-voltage, d.c. switchgear. The control-system complexity naturally increases with the number of modules in the system.

Thrustor performance characteristics and power requirements of interest to propulsion-system design are presented in this paper; these have been obtained from experimental operation of electron-bombardment thrustors. These data include recent measurements made with a nine-module array of 20-cm-diam thrustors and a single-module 50-cm-diam thrustor. Thrustor parameters are presented in terms of electric power consumption for each thrustor component (with current and voltage characteristics), as well as for the thrustor output parameters normally used for mission analysis. Thrustor control functions and electrical fault protection are described. The effects of thrustor efficiency, thrustor mass, and electric power-conversion system (power-conversion and power-conditioning are taken as a unit for the following discussion) on mission performance are illustrated by using a hypothetical Mars-orbiter mission as an example.

Electron-Bombardment Thrustor

Figure 1 is a cutaway sketch of an electron-bombardment thrustor with a 20-cm ion-beam diameter. The propellant (in this case, mercury) is vaporized in an electrically heated cavity and passes through a flow-metering orifice into the thrustor. The propellant passes through a flow distributor into the ion chamber, which contains the cylindrical anode and axially mounted cathode. The propellant is bombarded

Presented as Preprint 64-503 at the 1st AIAA Annual Meeting, Washington, D. C., June 29–July 2, 1964; revision received December 14, 1964.

* Head, Propulsion Systems Section. Member AIAA.

† Chief, Electrostatic Propulsion Branch; now Professor, Mechanical Engineering Department, Colorado State University, Fort Collins, Colo. Associate Fellow Member AIAA.

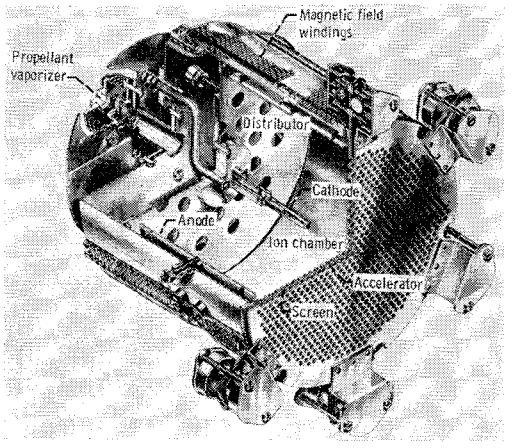

Fig. 1 Cutaway sketch of 20-cm-diam electron-bombardment thrustor.

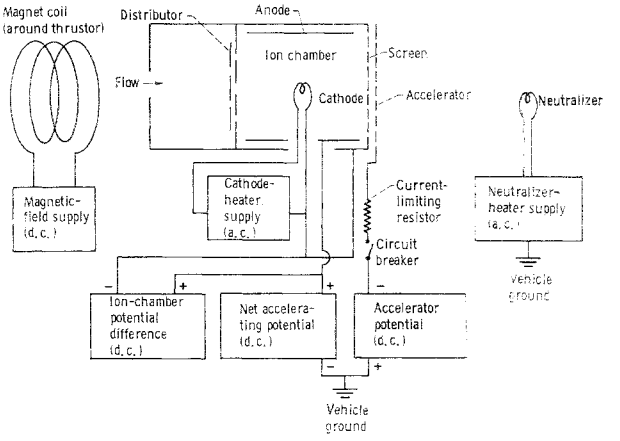

Fig. 2 Electron-bombardment thrustor electrical system.

by electrons emitted from the cathode, and some of it is ionized. An axial magnetic field prevents the emitted electrons from rapidly escaping to the anode, and escape to either end of the chamber is prevented by operating these ends at the same potential as the cathode. The ions that reach the downstream end of the ion chamber are focused by the screen grid and accelerated into an exhaust beam by the potential difference between the positive screen and negative accelerator grid. A neutralizer (not shown in Fig. 1) then neutralizes the current and charge of the exhaust beam. More information on this thrustor and its performance is contained in Refs. 1 and 3.

Six power supplies are required to operate the electron-bombardment thrustor (Fig. 2). The low-voltage, d.c. magnetic-field supply is used to produce the containment field for the ionizing electrons. The low-voltage, a.c. cathode-heater supply raises the thermionic emitter to the proper temperature. Another low-voltage, a.c. supply fulfills a similar function for the neutralizer. The discharge supply (about 50 v d.c.) provides the potential difference between the cathode and anode which accelerates the electrons emitted from the cathode to energies at which the propellant can become ionized. The two high-voltage d.c. supplies (net accelerating potential and accelerator potential) provide the potential difference between the screen and accelerator which focuses and accelerates the exhaust beam. The magnetic-field power supply can be eliminated if a permanent-magnet circuit is used to provide the electron containment field. Thrustors of this design are described in Ref. 6.

Electrostatic thrustors could be used for primary propulsion for a variety of spacecraft. These range from unmanned planetary probes that have propulsion power levels less than 100 kw to manned round-trip planetary vehicles with multimegawatt power-generation capabilities. The electron-bombardment thrustor can be scaled in size and in power level.[4] Experimental performance obtained with 20- and 50-cm-diam thrustors and the power requirements for these thrustors will be described in the next section. In subsequent sections, the control characteristics and electric breakdown protection of these thrustors will be discussed.

Thrustor Performance and Power Requirements

In this discussion, data from a 20-cm-diam thrustor designed for a 5000-sec specific impulse and a 50-cm-diam thrustor designed for a 9100-sec specific impulse are used as base points to determine the performance that can be expected from optimized electron-bombardment thrustors for the specific impulse range from 4000 to almost 10,000 sec.

Performance data for the 20-cm-diam thrustor described in this section were obtained from modules similar to the design shown in Fig. 1, except that a permanent-magnet circuit was employed.[6] The 50-cm-diam thrustor has four cathodes in the ionization chamber and magnetic-field windings. Thrustors of this size could also be operated with a permanent-magnet circuit.

For the purpose of thrustor array and large module tests, the component operating parameters were chosen to provide an accelerator electrode durability of 10,000 hr. This was done to provide realistic evaluations of thrustor performance parameters such as effective jet power density and thrustor mass to power ratios, as well as accurate thrustor component power ratios and electrical system loads. It is important to note here that 10,000-hr cathode durability has not yet been achieved; however, the power loss of the cathode is normally independent of lifetime and is only a function of the type and geometry of the unit employed. For missions requiring less than 10,000 hr, the module can be operated at a higher power level, thus taking advantage of the lower lifetime requirements.

Thrustor performance parameters used herein are as defined in Ref. 3. Thrustor efficiency η_{th} represents the efficiency with which the thrustor converts electric power and propellant mass into thrust. Thus

$$\eta_{\text{th}} = F^2/2\dot{m}_{\text{tot}}\mathcal{P}_{pc} \tag{1}$$

where F is thrust, $\dot{m}_{\text{tot}}$ is the total mass flow rate, and $\mathcal{P}_{pc}$ is the output from the power-conversion system; that is, $\mathcal{P}_{pc}$ is the total electric power input to the thrustor. The efficiency that must be used in mission analysis is η_{th}. Propellant utilization efficiency η_U defines the fraction of propellant that is ionized and accelerated and so defines propellant loss as

$$\eta_U \equiv \dot{m}_+/\dot{m}_{\text{tot}} \tag{2}$$

where $\dot{m}_+$ is the mass flow rate of ionized propellant. It is clear that

$$\eta_{\text{th}} = \eta_U F^2/2\dot{m}_+\mathcal{P}_{pc} \tag{3}$$

Figure 3 shows thrustor efficiency and propellant utilization efficiency plotted against specific impulse for both thrustors. The solid curves are the experimental data for the 20- and 50-cm-diam modules operated at optimum propellant utilization efficiency. The dashed curve is the optimum propellant utilization efficiency. The dot-dash curve is the maximum thrustor efficiency that can be expected from the electron-bombardment thrustor, assuming the experimental losses encountered in the 20-cm thrustor. More recent data with the 50-cm thrustor indicate that efficiencies higher than those predicted in Ref. 3 are achievable even at 10,000-hr operating conditions by use of more efficient cathodes and the larger size chamber. The larger chamber

appears to reduce wall losses. A value of thrustor efficiency of 88% was reported in Ref. 7 at 9000 sec.

The experimental performance of either thrustor falls below the expected performance when the thrustor is operated below the design specific impulse. The loss in efficiency is primarily caused by the reduction in the current-carrying capability of the fixed accelerator structure at the lower specific impulse. The accelerator lifetime and the specific impulse required for a given mission determine the accelerator geometry (screen and accelerator electrodes) with little room for compromise. The beam-current density and the spacing between screen and accelerator electrodes are determined from these considerations.[3] It has been found experimentally that the maximum aspect ratio (unsupported accelerator span divided by interlectrode spacing) that can withstand mechanical deformations caused by thermal effects is approximately 100.

Because the electrode spacing has been specified, the aspect ratio has the effect of limiting the module size, if no central support is used in the accelerator system. If the thrustor is operated below the design specific impulse, the current density is reduced because the net accelerating voltage is less, so that additional thrustors are required to produce the jet power required by the vehicle. Operating above the design specific impulse has the effect of using a thrustor that is smaller than the optimum size (diameter) and requires reductions in beam current of each module in order to maintain the required thrustor lifetime.

Preliminary design calculations have been made for a thrustor with a single support at the center of the screen and accel electrode plates. These calculations indicate that the thrustor exhaust-beam diameter could be increased to at least 100 cm, which would produce a module power of about 100 jet-kw at a specific impulse of 9000 sec. The use of center supports might also allow operation of a 50-cm-diam thrustor at a specific impulse of 5000 sec merely by decreasing the screen to accel electrode spacing.

It is also of interest, from a systems viewpoint, to determine the relative magnitudes of the component power loads and the current-voltage characteristics of each component as functions of specific impulse. Figure 4 displays such trends. Figure 4a shows the variation of magnet power, accelerator power, cathode-heater power, neutralizer-heater power, and discharge power with specific impulse for an optimized module. The curve for magnet power loss is dashed to indicate that permanent-magnet circuits can be substituted for the magnet windings, thus eliminating this power loss. The sum of the component powers of Fig. 4a are shown in Fig. 4b as a curve labeled "power losses." The effective jet power $P_{j,\mathrm{eff}}$ represents the jet power that is used in trajectory analysis and includes a correction for propellant loss. Thus

$$P_{j,\,\mathrm{eff}} = \eta_U P_j = \eta_{\mathrm{th}} \mathcal{P}_{pc} \qquad (4)$$

where the power P_j represents the ion-beam power that actually contributes to thrust. The ion-acceleration power P, shown in Fig. 4b, is the electric power consumed in accelerating ions. Therefore

$$\mathcal{P}_{pc} = P + \text{power losses} \qquad (5)$$

The effective jet powers $P_{j,\mathrm{eff}}$, shown as solid curves in Fig. 4b, are for the 20- and 50-cm-diam thrustor modules, which were designed for specific impulses of 5000 and 9100 sec, respectively. The dashed curve for $P_{j,\mathrm{eff}}$ represents the optimum values for thrustor modules designed for other specific impulses. These optimum values of $P_{j,\mathrm{eff}}$ were determined by using the data for the 20- and 50-cm-diam thrustors at design specific impulse as base points, and by using an interpolation formula relating ion-beam current to accelelectrode dimensions for a 10,000-hr durability. The interpolation formula was derived from relations given in Ref. 3. The ion-acceleration power P, shown in Fig. 4b, was determined from the optimum $P_{j,\mathrm{eff}}$, the power losses, and the thrustor efficiency η_{th} with Eqs. (4) and (5). The 20- and 50-cm-diam thrustor both have aspect ratios (beam diameter divided by electrode spacing) of 60, so the thrustor characteristics shown in Figs. 4–6 are for optimized thrustor designs with that aspect ratio.

The characteristics of several of the thrustor components (neutralizer and cathode heaters and magnet windings) are such that a significant fraction of the component power can be consumed without useful thrustor output. For example, two-thirds of the cathode-heater power may be required before the unit reaches emissive temperatures. Recognizing this restriction allows the statement to be made that, in general, the beam power, the accelerator power, and the discharge power increase approximately as the $\frac{5}{2}$ power of the specific impulse for small excursions from the design impulse (i.e., $\Delta I < 1000$ sec).

Figure 5 shows current and voltage characteristics for some of the components as specific impulse is varied. The positive net accelerating potential and negative accelerator potential are shown in Fig. 5a. The desired specific impulse and optimum propellant utilization efficiency naturally specify an exact net accelerating potential. The accelerator potential, however, can be operated at a variety of conditions. The solid upper curve represents the minimum negative potential that is required to keep electrons from the neutralizer from backstreaming into the positive thrustor. The dashed curve represents the potential, which has been

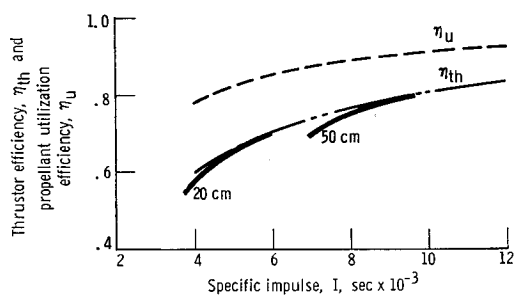

Fig. 3 Efficiency of 20- and 50-cm-diam electron-bombardment thrustors with mercury propellant and 10,000-hr design durability.

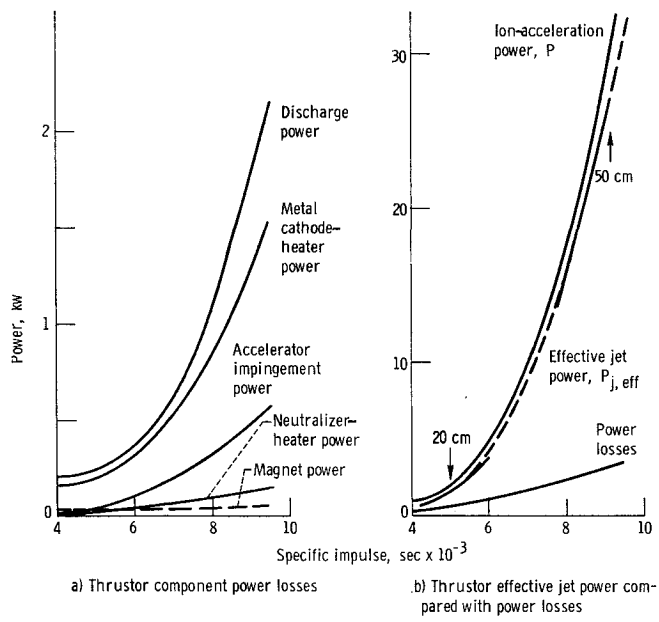

Fig. 4 Relative magnitudes of thrustor component power requirements for electron-bombardment thrustor with mercury propellant and 10,000-hr design durability.

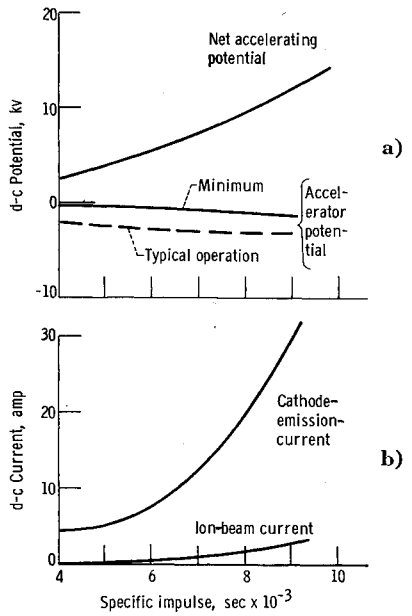

Fig. 5 Current and voltage requirements for several electron-bombardment thrustor components with 10,000-hr design durability.

found experimentally to yield stable operation with acceptable low accelerator impingement currents. High direct electrode impingement can result if the accelerator is operated at negative potentials above about 80% of the positive net accelerating potential. The sum of the beam and accelerator impingement currents is the current load at the net accelerating potential. The impingement current alone is the drain of the accelerator potential. The accelerator impingement current is typically 1% of the beam current. The variation of beam current with specific impulse (shown in Fig. 5b) was obtained from the curve for ion-acceleration power in Fig. 4b.

The neutralizer emission is, of course, kept equal to the beam current to provide over-all neutrality for the vehicle. A negative potential of a few volts below vehicle (space) potential will cause the neutralizer to emit the required electron current if the neutralizer is at the proper temperature. The other current shown in Fig. 5b, the cathode-emission current, is drawn at a constant discharge potential (which can be chosen between 35 and 50 v) regardless of module size.

As mentioned previously, the cathode and neutralizer heaters utilize low-voltage a.c. supplies. The power characteristic, shown in Fig. 4a, is the parameter of interest because it is determined by the size and type of cathode. The magnet supply, when used, can be designed to trade current for magnet coil turns to allow optimization of magnet and power-supply weights. Magnet coils in use normally require less than 10 amp d.c.

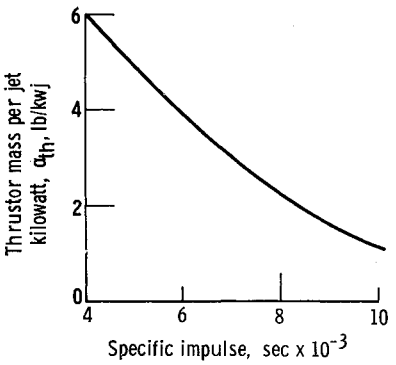

Fig. 6 Thrustor mass per jet kilowatt for electron-bombardment thrustor with 10,000-hr durability.

Figure 6 shows the variation of thrustor mass to power ratio α_{th} with specific impulse. The values range from 6.0 lb per effective jet-kw (beam power times propellant utilization efficiency) at 4000 sec to 1.1 lb per effective jet-kw at 10,000 sec. An array of nine 20-cm-diam thrustors has been operated successfully. The thrustors were arranged in three rows of three modules with 40-cm axial spacings. There were no significant interactions observed between thrustor modules that would interfere or detract from their performance. From this experiment, it may be concluded that the thrustor module performances presented so far should apply equally well to thrustor arrays for full-scale spacecraft.

Control Characteristics

Existing electrostatic thrustors must be operated at a specific impulse near the design value, since off-design operation results in substantial loss in thrustor performance. Because of this limitation, constant-specific-impulse trajectories with an optimum coast phase (power-coast-power) provide optimum mission performance.[3] With constant-specific-impulse operation, the net accelerating voltage supplied to the thrustor array is constant.

Unless thrustor redundancy is provided, permanent failure of an appreciable fraction of the thrustor array would require changing to a higher specific impulse in order to maintain full-rated power. Propellant reserve would be required for operation at off-optimum specific impulse.[8] In addition to the payload loss caused by the propellant reserve, the power-conversion system would require a variable voltage output for the ion-beam circuit. A redundancy of thrustors appears to be the preferable alternative and is assumed for the following discussion of controls characteristics.

In addition to the net accelerating voltage, the accelerator electrode voltage and the cathode-to-anode voltages also may be held constant for the whole array. The function of the control system would be to maintain the ion-beam current for each module at near the design value by controlling the cathode-emission current and the propellant flow rate in each thrustor. An example of a control function is correction for possible cathode deterioration. The cathode heating power required for a given cathode-electron-emission current may increase with time (e.g., because of physical damage from electric breakdowns). To maintain the ion-beam current at near the design value, the cathode heating power must be increased.[9,10] The additional current required for cathode heating must be taken from the emission current and the ion-beam current. The proper sharing of this current decrease is given by the static gain relation between emission current and ion-beam current. The ion-beam current will decrease somewhat, so a small reduction in propellant mass flow rate to the particular thrustor affected would be necessary in order to maintain optimum propellant utilization.

Steady-state control characteristics of the electron-bombardment thrustor with mercury propellant have been measured over a wide range of operating conditions.[11, 12] As shown in Figs. 7 and 8, these static gains are all well-behaved, continuous monotonic functions that do not have hysteresis effects, so that conventional closed-loop control-system-design principles apply. (The reader is referred to Ref. 11 for a detailed discussion of Figs. 7 and 8.) With the exception of the cathode and vaporizer heaters, the dynamic characteristics of the electron-bombardment thrustor have corner frequencies (break points) much higher than frequencies of interest for power-generation systems.[13] Both the cathode and the vaporizer heaters have corner frequencies much below those anticipated for power-generation systems. On the basis of these experimental measurements, it appears that control systems for electron-bombardment-thrustor arrays will have no insurmountable problems.

Electric Breakdown Protection

High-voltage electric breakdown in the thrustor can be of considerable significance to power-conversion components. Sparks or sustained arcs occur between electrodes in the thrustor, and these short circuits produce overcurrents which can damage the electrodes, solid-state rectifiers, and other components unless special precautions are taken in system design.

From the data reported in Ref. 14, it appears that a large fraction of electric breakdowns are self-quenching. The remaining fraction of breakdowns is sustained arcs that must be stopped with switches. To avoid needless power interruption, these switches must have an inherent time delay of milliseconds to allow self-quenching breakdowns to clear naturally.[15] (It is notable that this conclusion is in contradiction to the opinion of some who have stated that thrustor-breakdown switches must act with 36 μsec response.) Vacuum switches (commercially available) with suitable characteristics for this function are in regular use with the nine-module laboratory thrustor array described previously. With minor modifications, this type of switch can be made a small fraction of the thrustor weight.

The overcurrent magnitudes (for both self-quenching and switch-quenched breakdowns) can be impedance-limited if the breakdowns are forced to occur between the screen potential and accel electrode potential. By appropriate mechanical design, it appears that all of the high-voltage electric breakdowns can be forced to occur between the screen and accel circuits.[15] The accel electrode circuit (shown in Fig. 2) carries only 1–2% of the ion-beam current, and so a high-impedance, low-power resistor in the accel circuit can limit the magnitude of the overcurrent to a small value. With an appropriate capacitance in the power-conversion transmission cable, the suppressed overcurrent from high-voltage electric breakdowns should have a negligible effect on power-conversion components.

Primary Propulsion Systems

The potential merit of a particular thrustor design can be best assessed by incorporating that thrustor into a preliminary system design analysis. At present, electric powerplants and power-conversion systems for electric spacecraft do not exist, so that the analysis presented herein can only serve to indicate the performance required of those major components if the existing electron-bonbardment thrustor were used in a real propulsion system for an actual spaceflight mission.

A nuclear turboelectric powerplant with a turbine shaft power of 500 kws (s denotes shaft) and a weight of 7500 lb is assumed, so that $\alpha_{pp} = 15$ lb/kws. A power-conversion system consisting of an electric generator, transformers, rectifiers, controls, and switchgear is assumed which would have a specific weight of $\alpha_{pc} = 3.1$ lb/kwe (e denotes electric) based on power-conversion output power and an electric efficiency of $\eta_{pc} = 0.84$ (Ref. 16). The existing electron-bombardment thrustors described previously are assumed to be assembled into a thrustor array of a size commensurate with the power-generation system. Redundancy of components is not assumed. Merely for purposes of illustration, a Mars-orbiter mission is assumed where the electric spacecraft is launched with a chemical booster into a 300-naut-mile satellite orbit about Earth. The electric propulsion system then will propel the vehicle to a 350-naut-mile satellite orbit about Mars. An optimum date is assumed for leaving Earth. For this set of mission conditions, the optimum ratio of effective jet power to spacecraft starting mass is (depending upon trip time) about 0.012–0.020 kwj/lb (j denotes jet). A Saturn IB booster will deliver 28,500 lb into a 300-naut-mile Earth orbit, which results in a vehicle power to mass ratio of about 0.018 kw/lb; therefore, from the available boosters, the Saturn IB is the best choice.

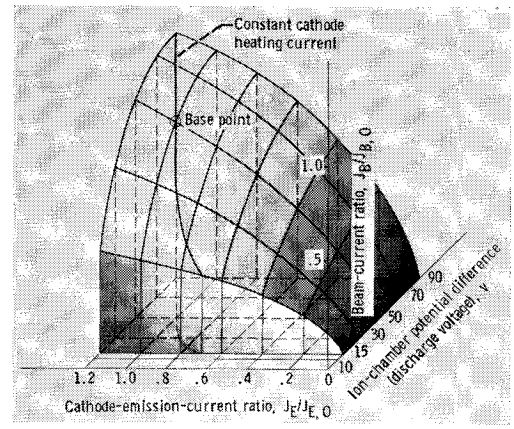

Fig. 7 Three-dimensional performance map showing static gains of beam-current ratio as function of ion-chamber potential difference and cathode-emission-current ratio.[11]

Propulsion-System Mission Performance

Optimum theoretical mission performance is obtained with the Irving-Blum trajectory along which full power is used continuously with unconstrained thrust magnitude and direction.[17,18] Specific impulse programs for the Irving-Blum trajectories have ranges far exceeding the capabilities of existing electrostatic thrustors.[3] Although the Irving-Blum trajectory could not be flown with existing thrustors, it does represent an ideal datum from which payload penalties chargeable to various system components and constraints can be shown. The Irving-Blum payloads shown in Fig. 9 are for a total propulsion-system specific weight of $\alpha_{ps} = 15$ lb/kw, for an optimum ratio of effective jet power to initial vehicle mass $P_{j,\mathrm{eff}}/M_0$ for each particular trip time and for a "single-stage" electric rocket. All of the other payloads in Fig. 9 are for constant-specific-impulse power-coast-power trajectories with optimized coast phases and with optimum specific impulse for each particular trip time. The procedure for determining optimum payload is shown in Fig. 10. The power-coast, power payloads were calculated from information in Ref.[18].

The payload penalty caused by the inability of the thrustor array to operate over a wide range of specific impulse is shown in region 1 in Fig. 9. This payload penalty is the

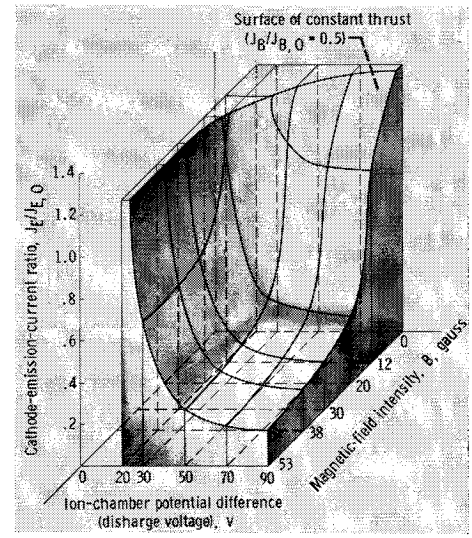

Fig. 8 Three-dimensional performance map showing surface of constant thrust in a function space of cathode-emission-current ratio, magnetic-field intensity and ion-chamber potential difference.[11]

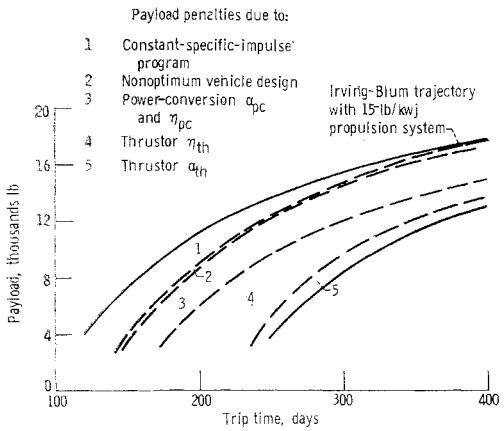

Fig. 9 Payloads for Mars-orbiter vehicle. Vehicle mass in 300-naut-mile Earth orbit, 28,500 lb (Saturn IB booster). Electric powerplant, 500 kw, 7500 lb. Power conversion, 3.1 lb/kw, 84% efficiency. Thrustor, existing electron-bombardment type. Final Mars satellite orbit, 350 naut miles.

difference between the Irving-Blum payload and the payload for power-coast-power trajectories with an optimum ratio $P_{j,\mathrm{eff}}/M_0$.

Since a particular powerplant and booster combination were chosen, the ratio $P_{j,\mathrm{eff}}/M_0$ is not optimum, and the payload penalty caused by the nonoptimum vehicle design is shown as region 2 in Fig. 9.

Payload penalty caused by the power-conversion system is shown by region 3 in Fig. 9. Not only does the power-conversion-system mass reduce the payload, but, in addition, the inefficiency of the power-conversion system reduces the electric power to the thrustor to $\mathcal{P}_{pc} = 420$ kwe.

The inefficiency of the thrustor array (shown in Fig. 3) further reduces the efficiency of the over-all propulsion system; that is, the effective jet power $P_{j,\mathrm{eff}}$ is substantially less than the power-conversion output power $\mathcal{P}_{pc}$. As described in Ref. 3, the effective jet power includes both electric power and propellant losses in the thrustors. Therefore

$$P_{j,\ \mathrm{eff}} = \eta_{\mathrm{th}}\mathcal{P}_{pc} = \eta_U\eta_P\mathcal{P}_{pc} = \eta_U\eta_P\eta_{pc}\mathcal{P}_{pp} \qquad (6)$$

where η_U and η_P are the thrustor propellant utilization efficiency and thrustor power efficiency, respectively. Payload penalty caused by thrustor inefficiency is shown by region 4 in Fig. 9. The payload penalty illustrated by region 5 is caused by the thrustor specific mass α_{th}, shown in Fig. 6. It is clear that considerable payload penalty is caused by the thrustor (regions 1, 4, and 5 in Fig. 9).

The net payload, after including all of the components weights and penalties, may be compared with the ideal Irving-Blum payload at each particular trip time to obtain an effective propulsion-system specific weight. On the basis of this comparison, the net payload (the lowest curve in Fig. 9) represents an effective propulsion-system specific weight over 50 lb/kwj at a trip time of 240 days and nearly 40 lb/kwj at a trip time of 400 days. When compared with the powerplant specific weight of 15 lb/kws, it may be said fairly that the sample system used here is severely affected by the power-conversion and thrustor components.

Power-coast-power trajectories are also possible with two-step specific impulse programs that might produce trajectories with payload fractions near those of the Irving-Blum trajectory.[3] If existing thrustors were used, two thrustor arrays would be required, that is, an array for each of the two specific impulse values. An inspection of Figs. 6 and 9 reveals that the increased weight of the second thrustor array might be less than the increase in payload for the faster trips. This observation depends upon the values of the two specific impulses and upon whether or not the power-conversion specific weight would be increased by the two-step accelerating voltage. Another factor to be considered is the possibility of using two different propellants, as analyzed in Ref. 3, in which case the same voltages might be used for both steps in the specific impulse program.

Another possibility for increasing payload capacity is the use of "multiple stages"; that is, the propulsion system would be modular, which would allow staging by dropping modules during the progress of the mission.[20] This concept amounts to successive reoptimization of the ratio $P_{j,\ \mathrm{eff}}/M_0$ throughout the flight. At the time of this writing, preliminary analyses show that staging has promise, but firm results are not yet available.

Table 2 Mars-orbiter, accel center support

Specific impulse, sec	Trip time, days	Effective jet power, kwj: Per thrustor module[a]	Effective jet power, kwj: Total vehicle	Number of 50-cm-diam thrustor modules with center support
4000	260	7.6	252	33
6000	330	14.1	294	21
8000	420	21.6	319	15

[a] Corrected for thrustor durability equal to trip time.

Thrustor Arrays for Electric Spacecraft

The mechanical design and detailed circuit design of thrustor arrays are also of interest in evaluating the merits of a particular thrustor. Both of these design problems depend strongly upon the number of thrustor modules required for the array and upon the ratio of effective jet power to total frontal area $P_{j,\mathrm{eff}}/A_{\mathrm{mod}}$ of a thrustor module.

The effective jet power per module for the 20- and 50-cm sizes of the mercury electron-bombardment thrustor is shown in Fig. 4b. The mission analysis described in the preceding section involved finding the optimum specific impulse for each particular trip time. This was done graphically for each of the payload curves shown in Fig. 9. Graphical optimization to obtain the final payload (i.e., the lowest curve) in Fig. 9 is displayed in Fig. 10. The number of modules

Table 1 500 kwe Mars-orbiter, existing thrustors

Specific impulse, sec	Trip time, days	Effective jet power, kwj: Per thrustor module[a]	Effective jet power, kwj: Total vehicle	Number of thrustor modules: 20-cm diam	Number of thrustor modules: 50-cm diam
4000	260	0.97	252	260	...
6000	330	4.5	294	65	...
8000	420	16.7	319	...	19

[a] Corrected for thrustor durability equal to trip time.

Table 3 Mars-orbiter, increased diameter

Specific impulse, sec	Trip time, days	Module diameter, cm	Effective jet power, kwj: Per thrustor module[a]	Effective jet power, kwj: Total vehicle	Number of modules with diameter equal to 200 times electrode spacing
4000	260	50	7.6	252	33
6000	330	94	49.5	294	6
8000	420	144	180	319	1.8

[a] Corrected for thrustor durability equal to trip time.

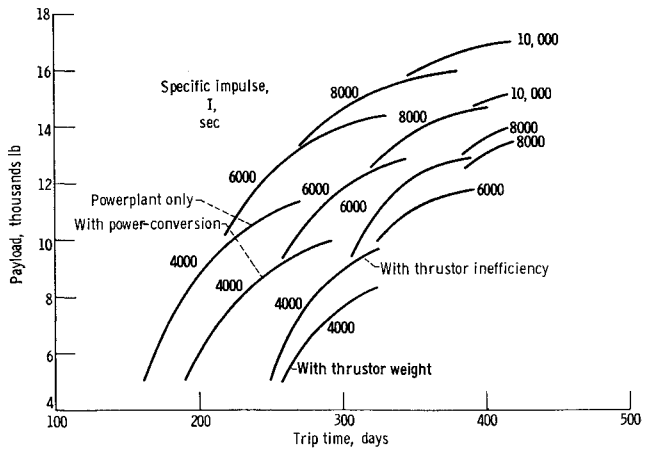

Fig. 10 Graphical optimization used to obtain payloads shown in Fig. 9. (Thrustor weight corrected for durability equal to trip time.)

required for each specific impulse shown in Fig. 10 is obtained simply from the total $P_{j,\text{eff}}$ for the vehicle and the $P_{j,\text{eff}}$ per module (see Table 1).

The possibility of increasing thrustor module size by the use of center supports has been discussed in the section "Thrustor Performance and Power Requirements." If a single center support between the grid and the accelerator electrodes were used in the 50-cm-diam thrustor, the grid-accelerator spacing could be reduced for specific impulses lower than 9100 sec. This reduction in accel length would provide a much higher effective jet power per module, so that a smaller number of thrustors could be used, as shown in Table 2.

Increased thrustor size through the use of center supports can be examined further by assuming that the thrustor diameter could be 200 times the grid-accelerator electrode spacing. Thus, with a center support, the aspect ratio of 100 discussed previously would be used for each thrustor. Thrustor arrays for the spacecraft being considered are shown in Table 3.

It is certainly evident that increased thrustor module size would greatly reduce complete thrustor array size and complexity. Whether modules with beam diameters as large as 144 cm can be operated successfully is a question to be answered by further research and development. Based on the work done so far, the eventual development of modules with power levels of several hundred kilowatts does appear feasible.

Conclusions

Two laboratory modules of mercury-propellant, electron-bombardment thrustors have been operated successfully in the specific impulse range from 4000–10,000 sec. On the basis of data from 20- and 50-cm-diam modules, performance and power requirements have been specified for optimized thrustors designed for other specific impulses. In both thrustor modules, the screen and accel electrode plates were supported only around the periphery, so that thrustor size was limited because of thermal warping of the plates. It is expected that, with the addition of a center support, allowable thrustor module diameter can be increased by at least a factor of 2.

No significant interactions were observed when nine of the 20-cm-diam modules were operated in an array. From this test, it is concluded that modules may be arrayed to whatever power level is required by the spacecraft. Experimental measurements of static and dynamic control characteristics show that the electron-bombardment thrustor is well behaved, so that no serious problems should arise in control system design. The use of a resistor and a vacuum switch with millisecond response in the accel electrode circuit will suppress current and voltage surges arising from electric breakdown in the thrustor. This suppression should be adequate to eliminate damaging interaction between the thrustor and the power-conversion system. Current estimates of thrustor weight, thrustor inefficiency, and power-conversion-system weight and inefficiency indicate that these factors would seriously reduce the payload for interplanetary missions.

References

[1] Kaufman, H. R., "The electron-bombardment ion rocket," Air Force Office of Scientific Research Symposium on Advanced Propulsion Concepts, Cincinnati, Ohio (October 1962).

[2] Mickelsen, W. R., "NASA Research on heavy-particle electrostatic thrustors," IAS Paper 63-19 (1963).

[3] Mickelsen, W. R. and Kaufman, H. R., "Status of electrostatic thrustors for space propulsion," NASA TN D-2172 (1964).

[4] Reader, P. D., "Scale effects on ion rocket performance," ARS J. **32**, 711–714 (1962).

[5] Molitor, J. H., "Application of ion thrustor motors in attitude and position control of satellites," Meeting of Combustion and Propulsion Panel of AGARD, Athens, Greece (July 1963).

[6] Reader, P. D., "Ion rocket with a permanent magnet," Astronaut. Aerospace Eng. **1**, 83 (October 1963).

[7] Reader, P. D., "Experimental performance of a 50-centimeter diameter electron-bombardment ion rocket," AIAA Preprint 64-689 (September 1964).

[8] Zola, C. L., "Trajectory methods in mission analysis for low-thrust vehicles," AIAA Preprint 64-51 (January 1964).

[9] Milder, N. and Kerslake, W. R., "Evaluation of filament deterioration in electron-bombardment ion sources," NASA TN D-2173 (1964).

[10] Kerslake, W. R., "Cathode durability in the mercury electron-bombardment ion thrustor," AIAA Preprint 64-683 (September 1964).

[11] Nakanishi, S., Pawlik, E. V., and Baur, C. W., "Experimental evaluation of steady-state control properties of an electron-bombardment ion thrustor," NASA TN D-2171 (1964).

[12] Pawlik, E. V. and Nakanishi, S., "Experimental evaluation of size effects on steady-state control properties of an electron-bombardment ion thrustor," NASA TN D-2470 (1964).

[13] Pawlik, E. V., unpublished data and analysis, NASA Lewis Research Center (1964).

[14] Stover, J. B., "Electric breakdown and arcing in experimental ion thrustor systems," AIAA Preprint 63-057 (1963).

[15] Stover, J. B., "Effect of thrustor arcing on ion rocket system design," AIAA Preprint 64-682 (September 1964).

[16] Doughman, C. L. and Stumph, F. C., "Space electric power systems study," Westinghouse Electric Corp., Fourth Quart. Progr. Rept. (August–November 1962).

[17] Irving, J. H. and Blum, E. K., "Comparative performance of ballistic and low-thrust vehicles for flight to Mars," *Vistas in Astronautics* (Pergamon Press, New York, 1959), Vol. III, pp. 191–218.

[18] Melbourne, W. G., "Interplanetary trajectories and payload capabilities of advanced propulsion vehicles," Jet Propulsion Lab., California Institute of Technology, Rept. TR 32-68 (March 1961).

[19] MacKay, J. S., unpublished analysis, NASA Lewis Research Center (1962).

[20] Edelbaum, T. N., "Multi-engine reliability for electric propulsion systems," ARS Paper 2388-62 (1962).